



A MODEL FOR THE ANALYSIS OF ELASTO-PLASTIC BUCKLING OF COMPRESSED COLUMNS

Nemanja Milekić¹, Milica Bendić¹, Stanko Ćorić¹, Zoran Perović¹

¹ Faculty of Civil Engineering

University of Belgrade, Bulevar kralja Aleksandra 73, 11000 Belgrade, Serbia

e-mail: nmilekic@grf.bg.ac.rs, mbendic@grf.bg.ac.rs, cstanko@grf.bg.ac.rs,
zperovic@grf.bg.ac.rs

Abstract:

Modern structures often use new technology materials as special high-strength steels. This is one of the reasons why cross-sections of structural members are smaller and structures are lighter than those built fifty years ago. Besides, there are new calculation methods that try to optimize material use and save money. Engineers today are faced with new challenges in terms of the design and construction process. Structures are often very slender and can be prone to loss of structural stability.

The most common example of such a slender element is columns. They are often subject to compression loading so stability can be a significant factor in element design. To build safe structures with optimized material use, it's very important to have a clear picture of element behavior in the pre-buckling and post-buckling phases. The nonlinear analysis could be very complex even for simple structures and because of that, different software is to be used for such tasks. In this paper, a simplified analytical model for the analysis of elasto-plastic buckling of compressed columns is illustrated.

Key words: stability analysis, stable symmetric bifurcation, elasto-plastic range, cantilever

1. Introduction

When we talk about the basics of bifurcation stability models, we usually mean symmetric stable bifurcation, symmetric unstable bifurcation, asymmetric bifurcation and snap through models. All these models are mainly analyzed in the theory of elasticity. This paper analyzes one of the models to check the difference between the system's buckling load and total load-bearing capacity to see what is happening in the post-buckling area of elasto-plastic materials.

Solving the problem of bifurcation stability in the elastic domain has been analyzed in different ways in literature [1-4]. There are several solving methods: 1) the bifurcation approach, 2) the energy approach and 3) the dynamic approach. The first method consists of having the equilibrium equations in a deformed configuration and determines the onset of buckling. In the second one, the change of the total potential energy of the system between two equilibrium states is used to derive the equations of equilibrium and to study its stability. In the third method, the equations of the system motion are established. Natural frequencies decreasing to zero correspond to the onset of instability [1].

These methods are generally well known in elastic theory and in this paper we will not show bifurcation paths and equations for all of them. We will deal only with the analysis of the stable symmetric bifurcation stability model since it is one of the most important and very common in practice (shells, rings, columns, etc. [5]).

Elasto-plastic hinged cantilever beam model is analyzed in pre buckling and post-buckling phase to determine equilibrium paths. Equilibrium paths are curves describing the relation between the displacements at some specific locations of the loaded structure and the load [1]. The hinged cantilever is a discrete, idealized model with rotational spring of stiffness k and pin connection at the end as shown in Figure 1. The load used is vertical concentrated compression force at the free end.

The main goal of this paper is to illustrate a simplified model for the analysis of elasto-plastic buckling of compressed columns.

2. Stable symmetric bifurcation of elastic system

To capture the post-buckling behavior and to determine the equilibrium paths, any bifurcation problem must be analyzed as fully non-linear. If we linearize the problem, we will solve equations more easily. However, if the determination of the post-buckling behavior is our goal non-linear calculations have to be used. From the linearized problem, the buckling load and bifurcation point can be determined.

For the subsequent calculations, the energy solution method will be used to find the bifurcation point. The total potential energy of the system in its initial configuration is Π_0 and is constant. Because we deal with the potential energy change, it will be eliminated from our equations.

In our analysis compressed column is modeled as a hinged cantilever with rotational spring (Fig.1). A change in potential energy between the two states, one initial and the other perturbed could be expressed as:

$$\Delta\Pi = \frac{1}{2}k\theta^2 - Pl(1 - \cos\theta) \quad (1)$$

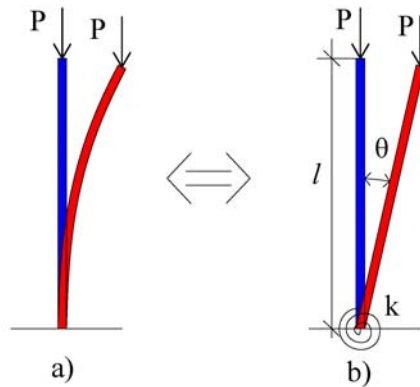


Fig. 1 Cantilever beam discrete model

The equilibrium paths correspond to configurations for which

$$\delta\Pi = 0 \rightarrow \frac{d\Pi}{d\theta} \equiv \Pi' = k\theta - Pl\sin\theta = 0 \quad (2)$$

Consequently, equilibrium configuration is achieved for:

$$\theta = 0 \quad \text{or} \quad P = \frac{k}{l} \cdot \frac{\theta}{\sin \theta}, \quad \theta \neq 0 \quad (3)$$

When we look at the Figure 2, the trivial equilibrium $\theta = 0$ corresponds to the initial straight configuration (no buckling) and that is the primary equilibrium path, prior to buckling.

The remaining equation $P = \frac{k}{l} \cdot \frac{\theta}{\sin \theta}$ or $\frac{P}{P_{cr}} = \frac{\theta}{\sin \theta}$, with notation $\frac{k}{l} \equiv P_{cr}$ corresponds to the secondary equilibrium branches which deviate from the vertical configuration since $\theta \neq 0$. The reason for the two branches to the left and to the right originates in the fact that angle θ could be positive or negative. In the bifurcation point the secondary equilibrium branch ($\theta > 0$ or $\theta < 0$) intersects initial path. The critical value of the load at this point $P = \frac{k}{l} = P_{cr}$ is called buckling load.

The stability of the equilibrium points and branches are investigated by observing the second variation of potential energy:

$$\delta^2 \Pi \rightarrow \frac{d^2 \Pi}{d\theta^2} \equiv \Pi'' = k - Pl \cos \theta \quad (4)$$

If the sign of the previous equation is positive the branch is stable and if it is negative the branch is unstable. If e.g. the second variation is zero (e.g. for $P = P_{cr}$) the higher derivatives have to be investigated.

By studying the second variation of Π it can be verified that the initial configuration ($\theta = 0$) is stable only for $P < P_{cr}$ while the secondary post-critical branch is stable in the whole domain [5].

In the next chapter, we will analyze the hinged cantilever model for elasto-plastic material. That model will have an imperfection, so structure imperfection must be introduced into previous equations to allow results comparison.

The geometric imperfection of the system will be taken into account through a small initial angle θ_0 . This initial imperfection will not apply any force in the rotational spring at the bottom of the model. If we find the change of potential energy, the next equations will be obtained:

$$\Pi = \frac{1}{2} k(\theta - \theta_0)^2 - Pl(1 - \cos \theta) \quad (5)$$

$$\Pi' = k(\theta - \theta_0) - Pl \sin \theta \quad (6)$$

$$\Pi'' = k - Pl \cos \theta \quad (7)$$

The equilibrium path is given as:

$$P = \frac{k}{l} \left(\frac{\theta - \theta_0}{\sin \theta} \right) \quad (8)$$

The equilibrium paths are stable ($\Pi'' > 0$) but for $P \rightarrow P_{CR}$ deformation from the engineering point of view is in most cases unacceptably large. If the above equation is linearized ($\sin \theta \approx \theta$), a well-known linearized response is obtained (when $P \rightarrow P_{CR}$ then θ tends to infinity).

Stable systems as one presented in this paper are not significantly affected by geometrical imperfections as unstable systems are. The impact of geometric imperfections is best seen through the comparison of limit load and critical bifurcation load of perfect systems. If the limit load for the system with small imperfection is much lower than the bifurcation load of the perfect

system, it means that structure is very sensitive to imperfections. Those kinds of structures are called imperfection sensitive and their load carrying capacity reduction can be very serious.

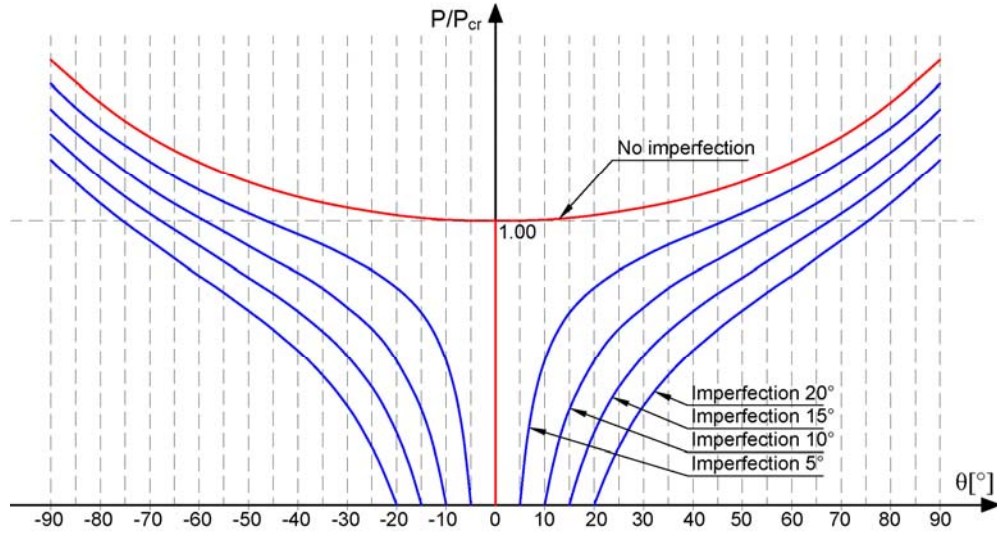


Fig. 2. Symmetric stable bifurcation of the elastic system

4. Stable symmetric bifurcation of elasto-plastic system with imperfection

The problem being analyzed is shown in the Figure 3:

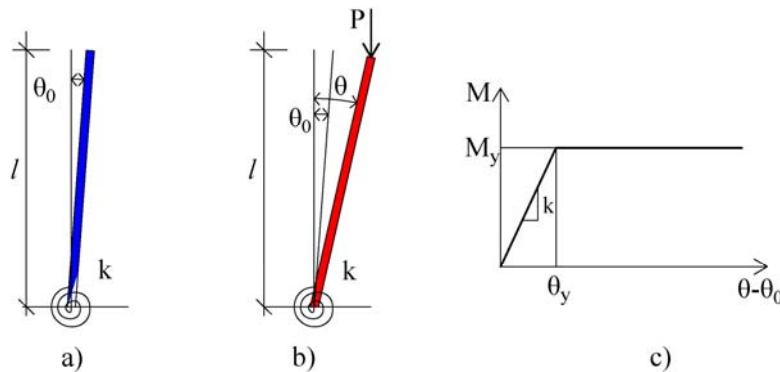


Fig. 3 Elasto-plastic system a) Initial state b) Deformed state c) $M - (\theta - \theta_0)$ diagram

In the elasto-plastic system shown in the Figure 3, the moment in the spring increases with angle θ , until the moment of plasticity at the angle θ_y is reached. After that, the moment in the spring remains constant with increasing angle θ .

The following relations can be determined from equilibrium state of the system:

$$P \cdot l \cdot \sin \theta = \begin{cases} k \cdot (\theta - \theta_0) & \text{za } \theta \leq \theta_0 + \theta_y \\ k \cdot \theta_y & \text{za } \theta > \theta_0 + \theta_y \end{cases} \quad (9)$$

$$P = \begin{cases} P_{cr} \cdot \frac{(\theta - \theta_0)}{\sin \theta} & \text{za } \theta \leq \theta_0 + \theta_y \\ P_{cr} \cdot \frac{\theta_y}{\sin \theta} & \text{za } \theta > \theta_0 + \theta_y \end{cases} \quad (10)$$

To solve equations (10) it is necessary to determine angle θ_y . This is the angle at which the rotational spring reached its full capacity and a plastic hinge is formed. To determine θ_y , the condition of full plasticity in the fixed end must be used:

$$\left(\frac{N}{N_p} \right)^n + \frac{M}{M_p} = 1 \quad (11)$$

The expression (11) determines the condition of full plasticity. It should be noted that with this equation the beginning of the plastification of the cross-section is equalized with full plastification. In this paper rectangular cross-section is used, so the value of n used in equation (11) is equal to 2 [6]. In (11) individual members are:

$$\begin{aligned} N &= P \\ M &= P \cdot l \cdot \sin(\theta) = P \cdot l \cdot \sin(\theta_0 + \theta_y) \\ N_p &= b \cdot d \cdot \sigma_y \\ M_p &= W_p \cdot \sigma_y \end{aligned} \quad (12)$$

where N_p is rectangular cross-section axial plastic capacity, M_p is rectangular cross-section moment plastic capacity and σ_y is yield strength of material.

If the values for P from (10) are inserted into (11), the equations for rectangular cross-section and $\theta = \theta_0 + \theta_y$ can be obtained as:

$$\left(\frac{P_{cr} \cdot \theta_y}{\sin(\theta_0 + \theta_y) \cdot N_p} \right)^2 + \frac{P_{cr} \cdot l \cdot \theta_y}{M_p} = 1 \quad (13)$$

If $P_{cr} = \frac{k}{l}$, then previous equation can be written as:

$$\left(\frac{k \cdot \theta_y}{l \cdot \sin(\theta_0 + \theta_y) \cdot N_p} \right)^2 + \frac{k \cdot \theta_y}{M_p} = 1 \quad (14)$$

There are several suggestions in the literature on how to calculate rotational spring stiffness when analyzing such models. In [7] the rigidity is adopted starting from Euler's critical buckling force:

$$P_{cr} = \pi^2 \frac{EI}{(2l)^2} \quad P_{cr} = \frac{k}{l} \quad \rightarrow \quad k = \pi^2 \frac{EI}{4l} = 2.46 \frac{EI}{l} \quad (15)$$

When the values for N_p and M_p are inserted in (14), it is obtained:

$$\left(\frac{2.46Eb^2}{12l^2 \cdot \sigma_y} \right)^2 \frac{\theta_y^2}{\sin^2(\theta_0 + \theta_y)} + \frac{2.46E \cdot b}{3l \cdot \sigma_y} \theta_y = 1 \quad (16)$$

It can be concluded that for a cross-section of a rectangular shape, the angle depends on the type of material from which the rod was made, on the minimal dimension of the cross-section, imperfection and the length of the rod.

4. Numerical analysis

In this analysis it is assumed that the rod is made of steel with characteristics: $E = 210\text{GPa}$, $\sigma_y = 240\text{MPa}$. So, the equation (16) can be presented as:

$$\left(179.38 \frac{b^2}{l^2} \right)^2 \frac{\theta_y^2}{\sin^2(\theta_0 + \theta_y)} + 717.50 \frac{b}{l} \theta_y = 1 \quad (17)$$

The several different cases of the ratio between cross-section width b and member length l are varied here. In doing so, b is kept constant and the value of l is varied. The value of the angle θ_y is determined by an iterative procedure so as to satisfy the above equation.

First case: $b=1\text{cm}$ and $l=10\text{cm}$

$$1.31 \frac{\theta_y^2}{\sin^2(\theta_0 + \theta_y)} + 71.75 \theta_y = 1 \quad (18)$$

If it is assumed that $\theta_0 = 5^\circ$, for the considered case, yielding occurs already at the value of $\theta_y \approx 1^\circ$. This is the consequence of the small height of the column so that the force P increases significantly before the angle reaches θ_y .

In the next case, the dimensions $b=1\text{cm}$ and $l=100\text{cm}$ are taken into account. If $\theta_0 = 5^\circ$, yielding occurs at the value of $\theta_y \approx 8^\circ$. It is clear that the deformability of the column is increased significantly with its height.

It is also considered the case of a slender rod with dimensions $b=1\text{cm}$ and $l=200\text{cm}$. Then the value of θ_y is obtained as approximately 16° . Previous considerations have shown that by increasing column height the first term of expression (17) (which shows the influence of axial force on plastification) loses its significance, and the second term becomes dominant.

Besides that those cases exposed that the increase in height of column directly affects the increase in deformability, the decrease in the stiffness of the springs and that the plastic yielding occurs at higher angles of rotation. However, although the rotation angles are larger, the plastic yielding occurs at a lower value of the force P , because of the high eccentricity of the load.

Table 1 gives the values of the maximum axial force that the analyzed model can bear until entering the plastic area, as well as the change in axial force with increasing angle θ in the plastic area. The same material parameters were adopted in the analysis as in the previous consideration but now angle θ_y is fixed at the value of 20° . The load-bearing capacity values are marked in green, and the force values in the plastic area are marked in gray.

λ	50				100				150				
P_{cr} [kN]	82.82				20.71				9.20				
θ_y [°]	20				20				20				
P [kN]	θ_0 [°]												
	0	5	10	15	0	5	10	15	0	5	10	15	
θ [°]	5	82.93	/	/	/	20.73	/	/	/	9.21	/	/	/
	10	83.24	41.62	/	/	20.81	10.41	/	/	9.25	4.62	/	/
	15	83.77	55.85	27.92	/	20.94	13.96	6.98	/	9.31	6.21	3.10	/
	20	84.53	63.39	42.26	21.13	21.13	15.85	10.57	5.28	9.39	7.04	4.70	2.35
	25	68.40	68.40	51.30	34.20	17.10	17.10	12.83	8.55	7.60	7.60	5.70	3.80
	30	57.82	57.82	57.82	43.36	14.45	14.45	14.45	10.84	6.42	6.42	6.42	4.82
	35	50.40	50.40	50.40	50.40	12.60	12.60	12.60	12.60	5.60	5.60	5.60	5.60
	40	44.97	44.97	44.97	44.97	11.24	11.24	11.24	11.24	5.00	5.00	5.00	5.00
$(P_{max} - P_{cr})/P_{cr}$	2%	-17%	-30%	-39%	2%	-17%	-30%	-39%	2%	-17%	-30%	-39%	

Table 1. Comparison of maximum and critical load in elasto-plastic analysis of systems with different degrees of imperfection and slenderness.

Obtained results show that for $\theta_y = 20^\circ$ the load-bearing capacity for the perfect system is 2% higher than Euler's critical force, and that increase is unrelated to the slenderness of the system.

In addition, it can be seen from the table that as the slenderness increases, the value of the maximum force that the system can receive disproportionately decreases. Also, with the increase of imperfection, a decrease in the load-bearing capacity of the system is clearly observed.

Based on the analysis conducted through Table 1 and Figure 2, parameters for Figure 4 are implemented. Equilibrium paths for $\theta_y = 20^\circ$ of the perfect system and system with the imperfection of $\pm 5^\circ$, $\pm 10^\circ$, $\pm 15^\circ$ and $\pm 20^\circ$ are given. So, the difference between the critical buckling force and the load-bearing capacity of the system can be seen.

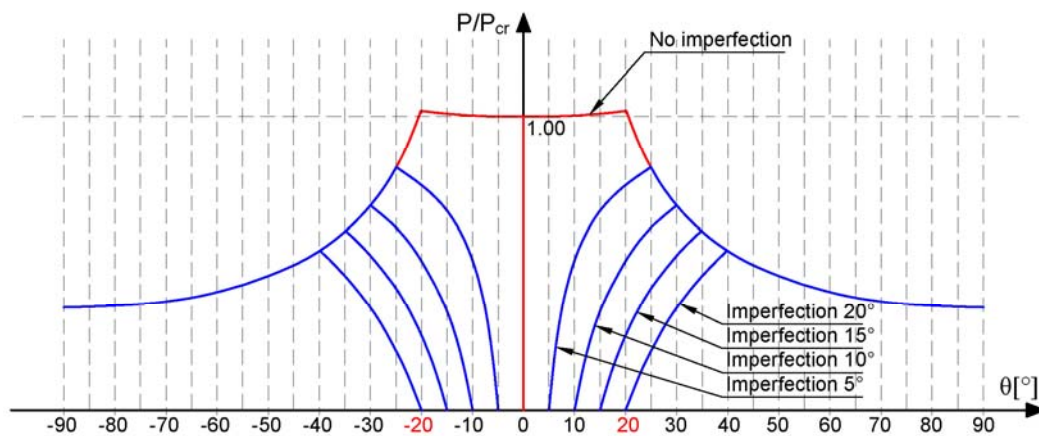


Fig. 4. Equilibrium paths for the elasto-plastic system without imperfection and with different values of imperfections, for yielding angle of $\theta_y = 20^\circ$

If a case without imperfection is observed, it can be detected that the rod remains vertical until it bends under the effect of critical axial load. If the imperfect system is analyzed it could be seen that the load-bearing capacity of the system decreases as imperfection increases.

The appearance of a plastic hinge occurs on the secondary path. After plastification, the slope of θ - P route becomes negative, which suggests that the system is in a state of unstable equilibrium. It could be observed that the axial load during the formation of the plastic hinge is higher than the one that causes the loss of stability, although the example shown that the difference is small.

It should be emphasized that with very short columns it can occur that $N_p < P_{cr}$ which means that the critical load is determined by plastification, and not buckling.

5. Conclusions

This paper analyzes a simplified model for the buckling of compressed cantilever columns. The model is based on a rigid rod with an elasto-plastic rotational spring. In the case of an elastic rod in the post-critical domain, the rod is still in a state of stable equilibrium (stable symmetric bifurcation). However, when $P \rightarrow P_{cr}$ displacements in the post-critical region are very large, so in the engineering sense a "loss of stability" term can be used, although strictly speaking the equilibrium states are stable. The response of the elasto-plastic system shows what happens with real compressed columns. Plastification is conditioned by the size of the initial imperfection. The fracture of the member corresponding to the full plastification of the cross-section is characterized by a sudden drop in force with an increase in displacements. For slender columns, the influence of axial force at cross-section plastification is minor by the rule. Presented analysis shows that after the point in which plastic hinge has formed the state of stable equilibrium no longer exists. The difference between this model and the real cantilever column is that the plastification of the cross-section is gradual, so there is no "spike" on the graph shown in Figure 4, but that part is rounded.

References

- [1] Baroudi Dj., *Elastic Stability of Structures*, Aalto University, Espoo, Finland, 2020.
- [2] Hjeltnad D., *Fundamentals of structural mechanics*, Springer Science+Business Media, 2005.
- [3] Jaguljnjak Lazarević A., Mario U., Čengija A., *Fundamental models of structural stability*, The Mining-Geology-Petroleum Engineering Bulletin, 0.17794/rgn.2017.2.5, 2017.
- [4] Timoshenko S., Gere J., *Theory of elastic stability*, McGraw Hill, 1961.
- [5] Thompson J.M.T., Hunt G.W., *A general theory of elastic stability*, John Wiley and Sons, 1973.
- [6] Mijalković M., Trajković M., Milošević B., *Limit analysis of beams under combined stresses*, Architecture and Civil Engineering Vol. 6, No 1, 2008.
- [7] Cao K., Yao-Jie G., Xu J., *Buckling Analysis of Columns Ended by Rotation-stiffness Spring Hinges*, International Journal of Steel Structures 16(1):1-9, 2016.